

Journal of Materials Chemistry A

Accepted Manuscript



This is an *Accepted Manuscript*, which has been through the Royal Society of Chemistry peer review process and has been accepted for publication.

Accepted Manuscripts are published online shortly after acceptance, before technical editing, formatting and proof reading. Using this free service, authors can make their results available to the community, in citable form, before we publish the edited article. We will replace this *Accepted Manuscript* with the edited and formatted *Advance Article* as soon as it is available.

You can find more information about *Accepted Manuscripts* in the [Information for Authors](#).

Please note that technical editing may introduce minor changes to the text and/or graphics, which may alter content. The journal's standard [Terms & Conditions](#) and the [Ethical guidelines](#) still apply. In no event shall the Royal Society of Chemistry be held responsible for any errors or omissions in this *Accepted Manuscript* or any consequences arising from the use of any information it contains.

Highly Porous and Photoluminescent Pyrene-Quinoxaline-Derived Benzimidazole-Linked Polymers

Suha Altarawneh[†], Lamia Nahar[†], Indika U. Arachchige^{*†}, Ala'a O. El-Ballouli[‡], Kassem M. Hallal[‡], Bilal R. Kaafarani^{*‡}, Mohammad Gulam Rabbani^{†§}, Ravi K. Arvapally[†] and Hani M. El-Kaderi^{*†}

[†]Department of Chemistry, Virginia Commonwealth University, Richmond, Virginia 23284-2006, United States

[‡]Department of Chemistry, American University of Beirut, Beirut 1107-2020, Lebanon

[§]Present address: Department of Chemistry and Engineering Physics, University of Wisconsin-Platteville, Platteville, WI 53818

ABSTRACT

Two highly porous and semiconducting pyrene-quinoxaline-derived benzimidazole-linked polymers have been synthesized and fully characterized. The polymers have high surface area ($S_{\text{BET}} = \sim 950 \text{ m}^2 \text{ g}^{-1}$) while their electronic structure studies reveal bandgaps in the semiconducting range (2.02 and 2.16 eV) and emissions in the orange-red region (600 and 630 nm). The high surface area and optical properties make these polymers very interesting for gas storage, optoelectronics, and sensing applications.

1. Introduction

In recent years, there has been great interest in the designed synthesis of porous organic polymers (POPs) due to their potential in a broad range of applications including catalysis, gas storage and separation, optoelectronics, and sensing.¹⁻¹⁰ Among POPs are benzimidazole-linked polymers (BILPs) that have high porosity and remarkable selectivity for capturing carbon dioxide from gas mixtures typically found in flue gas and natural gas.¹¹⁻¹⁵ Although porous benzimidazole-containing polymers have been explored for catalysis,^{16, 17} proton-conductivity,¹⁸ and selective gas uptake,^{11-15, 19-21} surprisingly their optical properties have received little attention.²²⁻²⁴ Furthermore, embodiment of N-heterocyclic building units into π -electron rich molecules or conjugated polymers is a well-known strategy for tuning their optical properties and electronic structures.²⁵⁻³⁴ For example, introducing N-atoms into acene fragments lead to enhanced stability and prevent photooxidation and Diels-Alder reaction.³⁵⁻³⁸ In a seminal review, Mateo-Alonso described the recent developments in the field of pyrene-fused pyrazaacenes.³⁹ Microporous materials containing quinoxalinophenanthrophenazine (QPP) chromophore have been recently reported with surface areas of $754 \text{ m}^2 \text{ g}^{-1}$ and $776 \text{ m}^2 \text{ g}^{-1}$.^{26, 34} A hole-mobility as high as $4.2 \text{ cm}^2 \text{ V}^{-1} \text{ s}^{-1}$ was recorded for QPP covalent organic frameworks.³⁴ In addition, the imine-N provides sites for hydrogen-bonding and thereby aids molecular aggregation or substrate binding.⁴⁰⁻⁴² Additional intermolecular interactions can also arise from the ambipolar imidazole units that can act as both H-donor and acceptor facilitating solid-state packing.⁴³ Therefore, integrating novel optical properties into POPs in general and BILPs in particular, without compromising porosity would be vital for their future multifaceted applications.

In this study, we report for the first time the synthesis of highly porous pyrene-quinoxaline-derived BILPs and investigate their electronic structure by absorption-

photoluminescence spectroscopy. In addition to their high porosity ($S_{\text{ABET}} = \sim 950 \text{ m}^2 \text{ g}^{-1}$) the polymers exhibit semiconducting properties (2.02 and 2.16 eV) and emit with peak maxima in the orange-red region (600 and 630 nm).

2. Experimental Methods

All chemicals were purchased from commercial suppliers (Sigma Aldrich, Acros Organics and Frontier Scientific) and used without further purification, unless otherwise noted. *N,N',N'',N'''*-(2,11-di-*tert*-butylquinoxalino[2',3':9,10]phenanthro[4,5-*abc*]phenazine-6,7,15,16-tetrayl)tetrakis(4-methylbenzenesulfonamide)-referred to as TQPP-NHTs,⁴⁴ 1,3,5,7-tetrakis(4-formylphenyl) adamantane,⁴⁵ and 1,2,4,5-tetrakis(4-formylphenyl) benzene¹¹ were prepared according to literature procedures. Air-sensitive samples and reactions were handled under an inert atmosphere of nitrogen using Schlenk line technique. Elemental microanalyses were performed at the Midwest Microlab, LLC. ¹H and ¹³C NMR spectra were obtained on a Varian Mercury-300 MHz NMR spectrometer. ¹³C cross-polarization magic angle spinning (CP-MAS) NMR spectra for solid samples were taken at Spectral Data Services, Inc. Thermogravimetric analysis (TGA) was carried out using a TA Instruments Q-5000IR series thermal gravimetric analyzer with samples held in 50 μL platinum pans under nitrogen (heating rate 10 $^{\circ}\text{C}/\text{min}$). For scanning electron microscopy imaging (SEM), samples were prepared by dispersing the material onto a sticky carbon surface attached to a flat aluminum sample holder. The sample was then coated with platinum at 6×10^{-5} mbar for 60 seconds before imaging. Images were taken on a Hitachi SU-70 Scanning Electron Microscope. Powder X-ray diffraction data were collected on a Panalytical X'pert pro multipurpose diffractometer (MPD). Samples were mounted on a sample holder and measured using Cu $K\alpha$ radiation with a 2θ range of 1.5-35. FT-IR spectra were

obtained as KBr pellets using Nicolet-Nexus 670 spectrometer. Sorption experiments were collected using a Quantachrome Autosorb IQ2 analyzer.

UV-Visible absorption spectra were recorded using a Cary 6000i UV-Vis-NIR spectrophotometer (Agilent Technologies) by using 10 mm quartz cuvettes.⁴⁶ For the solution UV-Visible absorption and emission spectra, ~0.0035 g polymers were dispersed in DMF and sonicated for 2-3 min, and let the solution to settle down within couple of minutes. The yellow color supernatant was used to carry out the absorption measurements. UV-Vis spectra of the powdered polymers were acquired by employing the Diffuse reflectance (DRA) accessory equipped with an integrating sphere in the Cary 6000i UV-Visible spectrophotometer. The powdered polymer was pressed on top of barium sulfate (as background) surface to perform the band gap measurements. The data obtained from DRA was converted to absorption utilizing the Kubelka-Munk function.^{47, 48} Solution photoluminescence of the polymers were performed using a Cary Eclipse Fluorescence spectrophotometer (Agilent Technologies) with 10 nm excitation and emission slit in a quartz optical cell. Excitation and emission spectra are corrected using the software provided and the same are used for Stokes shift calculation. Same solution is used for UV-Visible and photoluminescence measurements. Emission measurements of the powdered polymers were carried out at liquid N₂ temperature (77 K) using a cryogenic cold trap. Quantum yield measurements were carried out using a Cary 6000i UV-Vis-NIR spectrophotometer and Cary Eclipse Fluorescence spectrophotometer (Agilent Technologies). About 0.001g of polymers sample was dispersed into ethanol solution and the absorption and emission were compared to Rhodamine 101.

Synthesis of 2,11-di-tert-butylquinoxalino[2',3':9,10]phenanthro[4,5-abc]phenazine-6,7,15,16-tetraamine (TQPP-NH₂)

A 50 mL round bottom flask was charged with concentrated H₂SO₄ (5.0 mL) and degassed by bubbling with N₂ for 30 min then TQPP-NHTs⁴⁴ (200 mg, 0.167 mmol) was added under vigorous stirring. The resulting solution was stirred for 18 h at room temperature then poured into ice (~30 g). After filtration over a medium glass frit the solid was washed with water and neutralized with 0.5 M NaOH. The solid product was finally washed with methanol and dried under vacuum to afford TQPP-NH₂ as a fine red powder (92 mg, 0.159 mmol, 95% yield). ¹H NMR (DMSO-*d*₆, 300 MHz) 9.48 (s, 4H), 7.22 (s, 4H), 6.12 (s br, 8H, NH₂), 1.65 (s, 18H, CH₃). TQPP-NH₂ was used in subsequent reactions without further purification.

Synthesis of BILP-17

A 100 mL Schlenk flask was charged with (60 mg, 0.104 mmol) of TQPP-NH₂ and 30 mL of anhydrous DMF. The solution was cooled to -30 °C and HCl (0.4 M, 2 mL, 0.8 mmol) was added to the solution and stirred for 1 hr. 1,3,5,7-Tetrakis(4-formylphenyl) adamantane (29.0 mg, 0.052 mmol) in 25 mL anhydrous DMF was added dropwise. The temperature was maintained around -30 °C until the brown solid product formation completed and then raised to RT and kept for overnight. The flask containing the reaction mixture was bubbled with air for 15 minutes and capped. The reaction mixture was then heated in an oven at 130 °C (0.5 °C/min) for 3 days to afford a brownish polymer which was isolated by filtration over a medium glass frit. The product was immersed in DMF (20 mL overnight) then acetone (20 mL). The product was filtered and dried under vacuum at 120 °C and 1.0 x 10⁻⁵ Torr for 20 hours to give **BILP-17** as a brown solid

(41 mg, 79%). Anal. Calcd for $C_{55}H_{44}N_8 \cdot 6H_2O$: C, 65.6%; H, 4.97%; N, 11.13%. Found: C, 66.73%; H, 5.29%; N, 10.39%.

Synthesis of BILP-18

In a fashion similar to the preparation of **BILP-17**, treatment of TQPP-NH₂ (60.0 mg, 0.104 mmol) with 1,2,4,5-tetrakis(4-formylphenyl)benzene (25 mg, 0.051 mmol) in the presence of HCl (0.4 M, 2 mL, 0.8 mmol) afforded **BILP-18** as a yellow-brownish powder (37 mg, 74%). Anal. Calcd for $C_{45}H_{22}N_8 \cdot 3H_2O$: C, 65.17%; H, 4.5%; N, 11.48%. Found: C, 66.7%; H, 4.49%; N, 10.76%.

3. Results and Discussion

The pyrene-quinoxaline-derived BILPs were prepared by co-condensation reactions between aryl-*o*-aldehydes and 2,11-di-*tert*-butyl-6,7,15,16-tetraaminoquinoxalino[2'-3':9,10]phenanthro[4,5-*abc*]phenazine (TQPP-NH₂) in DMF according to our recently published procedure¹¹⁻¹⁵ as illustrated in Scheme 1. Scanning electron microscopy (SEM) revealed an agglomerated particles ca. 0.5-0.3 μm in size (Fig. 1A-B) while powder X-ray diffraction confirmed amorphous structures (Fig. S1, ESI). The thermal stability was obtained from the thermogravimetric analysis (TGA) which indicates that BILPs are thermally stable up to 400 °C under N₂ (Fig. S2, ESI). The chemically robust BILPs remained intact upon treatment with aqueous HCl and NaOH (4M). The chemical connectivity of BILPs was confirmed by FT-IR and solid-state ¹³C CP-MAS NMR. The FT-IR spectra for both BILPs (Fig. S3, A & B, ESI) contain broad bands at 3435 cm⁻¹ (N-H stretching), 3224 cm⁻¹ (hydrogen bonded N-H), and new bands at 1620 cm⁻¹ (C=N) of the imidazole and the phenazine moieties. The vibrations at 1620, 1480 and

1435 cm^{-1} are attributed to the skeleton of the imidazole ring. The ^{13}C CP-MAS spectra (Fig. S4, ESI) revealed characteristic peaks of the imidazole ring (NC(Ph)N) at ~ 151 ppm along with other peaks that correspond to the aryl units of BILPs,¹¹⁻¹⁵ while the sharp peaks around 25 and 31 ppm are corresponding to the *tert*-butyl-substituents on the pyrene core and the adamantane unit, respectively. The porosity of the new BILPs was evaluated by argon uptake measurements (Fig. 1C, Table 1). Both isotherms are fully reversible with a minor hysteresis consistent with the powdery nature of BILPs. The gradual uptake of Ar with increased pressure leads to Type II isotherms, which are expected because of the long nature of the organic linkers that tend to form flexible and interpenetrated frameworks. The “elastic” nature of the polymers can be beneficial for admitting gas molecules or ions into the pores for storage and sensing applications. The Brunauer-Emmett-Teller (BET) surface area was found to be $952 \text{ m}^2 \text{ g}^{-1}$ (**BILP-17**) and $947 \text{ m}^2 \text{ g}^{-1}$ (**BILP-18**) (Fig. S5, ESI). Our values are 22-26% higher than those reported previously in QPP porous materials.^{26,34} Pore size distribution (PSD) curves derived from the nonlocal density functional theory (NLDFT) were found to be centered about 8.3 \AA (**BILP-17**), and 5.5 \AA (**BILP-18**). Pore volume was calculated from single point measurements ($P/P_0 = 0.95$) and found to be 0.93 cc g^{-1} (**BILP-17**), and 0.76 cc g^{-1} (**BILP-18**).

4. Photoluminescence Study

To investigate the electronic structure of BILPs we have recorded the UV-Visible absorption, photoluminescence (PL), and photoluminescence excitation (PLE) spectra of the polymers and the corresponding tetra-amine monomers and the data are shown in Fig. 2. Both polymers exhibit well-defined absorption spectra when dispersed in DMF via sonication. The absorption spectrum of the **BILP-17** exhibits sharp excitonic features at 304, 340, and 451 nm along with a low

intensity absorption hump at 428 nm whereas that of **BILP-18** exhibits similar excitonic features at 297, 344, and 461 nm and a low intensity shoulder at 433 nm (Fig. 2A). In contrast, the corresponding monomer units dispersed in DMF display well-defined excitonic peaks at 315, 337, and 468 nm with a low intensity shoulder at 440 nm. Based on the literature reports on pyrene-fused azaacenes the absorption humps observed at 428, 433, and 440 nm for **BILP-17**, **BILP-18**, and the corresponding tetra-amine monomers can be assigned to $n-\pi^*$ electronic transitions.^{26, 30} Likewise, the sharp excitonic maxima observed at 340, 344, and 337 nm for **BILP-17**, **BILP-18**, and the monomers are likely to arise from $\pi-\pi^*$ optical transitions.^{48, 49} The relatively smaller changes in the solution absorption spectra of the polymers in comparison to monomer units suggest minimum or no change in the electronic structure upon polymerization. The solid state diffuse reflectance (converted to absorption) spectra of both polymers exhibit well-defined bandgap onsets in the visible spectrum that are significantly red shifted (Table 1, Fig. S6, ESI) compared to the tetra-amine monomer units (2.21 eV). The lower bandgaps observed in polymers in comparison to precursor monomers can be attributed to increased charge delocalization of the excitonic states, which can potentially create low energy electronic transitions upon polymerization.⁴⁹

When a solution of **BILP-17** is exposed to an excitation source of 448 nm (PLE maxima), a less intense orange-red emission with a peak maximum at 607 nm was observed (Fig. 2B). Moreover, the emission is found to be independent of the excitation energy (Figure S9, ESI). Similarly, the luminescence spectrum of the **BILP-18** in DMF exhibit an intense red emission with a peak maximum at 623 nm (PLE = 463 nm, Fig. 2B), which is independent of the energy of excitation (Fig. S9, ESI). In contrast, the corresponding tetra-amine units dispersed in DMF exhibit green emission with a peak maximum at 528 nm (PLE = 395 nm) along with a well-

defined vibronic pattern (Fig. 2B) suggesting the inherent molecular structure.⁵⁰ The Stokes shift of 5847 cm⁻¹ for **BILP-17** and 5547 cm⁻¹ for **BILP-18** clearly indicates significant changes in the exciton prior to radiative relaxation. Consistent with the bandgap measurements, the emission energy of **BILP-17** is found to be intermediate of those of the tetra-amine monomer and **BILP-18** likely due to the disruption of conjugation at the adamantane center. Nevertheless, the vibronic structure inherent in the monomer units was not observed in the emission spectra of both polymers, likely due to absence of molecular structure. This observation is consistent with the increased π - π conjugation in both polymers as a result of benzimidazole moiety formation. Quantum yield measurements were carried out relative to Rhodamine 101 in ethanol and showed values in the range of <0.1% and 9% for **BILP-17** and **BILP-18**, respectively. The improved quantum efficiency of **BILP-18** in comparison to **BILP-17** can be attributed to the increased charge delocalization in **BILP-18** due to the extended conjugation along the framework of polymer, which can potentially increase the probability of radiative recombination of the exciton.

5. Conclusion

We have demonstrated that a template-free co-condensation coupling reactions of 2D and 3D aryl-*o*-aldehydes with and 2,11-di-*tert*-butyl-6,7,15,16-tetraamino-quinoxalino[2'-3':9,10]phenanthro[4,5-*abc*]phenazine (TQPP-NH₂) afforded highly porous and semiconducting BILPs. The high surface area and porosity obtained in the BILP polymers along with the high PL quantum yields in the visible spectrum suggest that these materials are promising for gas or molecular sensing applications. Specific studies to test this premises are currently underway.

Supporting Information

Spectral characterization, porosity measurements, and electronic structure studies of BILPs. This material is available free of charge via the Internet at **.

AUTHOR INFORMATION

Corresponding Authors

iuarachchige@vcu.edu, bilal.kaafarani@aub.edu.lb, and helkaderi@vcu.edu

Acknowledgments

Research supported by the U. S. Department of Energy, Office of Basic Energy Sciences under award number (DE-SC0002576). S.A. thanks Tafila Technical University-Jordan for fellowship. B.R.K. thanks Petroleum Research Fund (PRF) of the American Chemical Society (Grant No. 47343-B10) and the Arab Fund Fellowship Program. I.U.A. thanks Petroleum Research Fund (PRF) of the American Chemical Society (Grant No. 52423-DNI10) and VCU for funding.

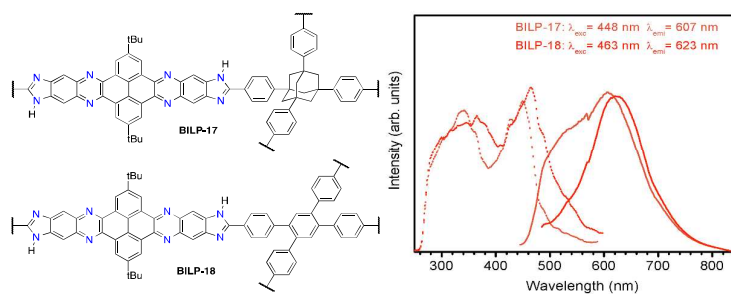
References

1. D. Wu, F. Xu, B. Sun, R. Fu, H. He and K. Matyjaszewski, *Chem. Rev. (Washington, DC, U. S.)*, 2012, 112, 3959-4015.
2. P. Kaur, J. T. Hupp and S. T. Nguyen, *ACS Catal.*, 2011, 1, 819-835.
3. X. Feng, X. Ding and D. Jiang, *Chem. Soc. Rev.*, 2012, 41, 6010-6022.
4. M. Dogru and T. Bein, *Chem. Commun.*, 2014, 50, 5531-5546.
5. Z. Xiang and D. Cao, *J. Mater. Chem. A*, 2013, 1, 2691-2718.
6. X. Zou, H. Ren and G. Zhu, *Chem. Commun.*, 2013, 49, 3925-3936.
7. S.-Y. Ding and W. Wang, *Chem. Soc. Rev.*, 2013, 42, 548-568.
8. P. Kuhn, M. Antonietti and A. Thomas, *Angew. Chem., Int. Ed.*, 2008, 47, 3450-3453.
9. (a) R. Dawson, A. I. Cooper and D. J. Adams, *Prog. Polym. Sci.*, 2012, 37, 530-563. (b) R. T. Woodward, L. A. Stevens, R. Dawson, M. Vijayaraghavan, T. Hasell, I. P. Silverwood, A. V. Ewing, T. Ratvijitvech, J. D. Exley, S. Y. Chong, F. Blanc, D. J. Adams, S. G. Kazarian, C. E. Snape, T. C. Drage and A. I. Cooper, *J. Am. Chem. Soc.*, 2014, 136, 9028-9035.
10. G. Li, B. Zhang, J. Yan and Z. Wang, *J. Mater. Chem. A*, 2014, DOI: 10.1039/c4ta04429k, Ahead of Print.
11. S. Altarawneh, S. Behera, P. Jena and H. M. El-Kaderi, *Chem. Commun.*, 2014, 50, 3571-3574.
12. M. G. Rabbani and H. M. El-Kaderi, *Chem. Mater.*, 2011, 23, 1650-1653.
13. M. G. Rabbani and H. M. El-Kaderi, *Chem. Mater.*, 2012, 24, 1511-1517.
14. M. G. Rabbani, T. E. Reich, R. M. Kassab, K. T. Jackson and H. M. El-Kaderi, *Chem. Commun.*, 2012, 48, 1141-1143.
15. M. G. Rabbani, A. K. Sekizkardes, O. M. El-Kadri, B. R. Kaafarani and H. M. El-Kaderi, *J. Mater. Chem.*, 2012, 22, 25409-25417.
16. B. Liu, T. Ben, J. Xu, F. Deng and S. Qiu, *New J. Chem.*, 2014, 38, 2292-2299.
17. X.-J. Zhang, N. Bian, L.-J. Mao, Q. Chen, L. Fang, A.-D. Qi and B.-H. Han, *Macromol. Chem. Phys.*, 2012, 213, 1575-1581.
18. J. A. Asensio, E. M. Sanchez and P. Gomez-Romero, *Chem. Soc. Rev.*, 2010, 39, 3210-3239.
19. M. Zhang, Z. Perry, J. Park and H.-C. Zhou, *Polymer*, 2014, 55, 335-339.
20. H. Yu, M. Tian, C. Shen and Z. Wang, *Polym. Chem.*, 2013, 4, 961-968.
21. Y.-C. Zhao, Q.-Y. Cheng, D. Zhou, T. Wang and B.-H. Han, *J. Mater. Chem.*, 2012, 22, 11509-11514.
22. J. D. Harris, C. Mallet, C. Mueller, C. Fischer and K. R. Carter, *Macromolecules*, 2014, 47, 2915-2920.
23. J. Weber, *ChemSusChem*, 2010, 3, 181-187.
24. S. W. Thomas, III, G. D. Joly and T. M. Swager, *Chem. Rev. (Washington, DC, U. S.)*, 2007, 107, 1339-1386.
25. G. Korotcenkov, S. D. Han and J. R. Stetter, *Chem. Rev. (Washington, DC, U. S.)*, 2009, 109, 1402-1433.
26. B. Kohl, F. Rominger and M. Mastalerz, *Org. Lett.*, 2014, 16, 704-707.
27. X. Feng, F. Iwanaga, J.-Y. Hu, H. Tomiyasu, M. Nakano, C. Redshaw, M. R. J. Elsegood and T. Yamato, *Org. Lett.*, 2013, 15, 3594-3597.
28. C. Tong, W. Zhao, J. Luo, H. Mao, W. Chen, H. S. O. Chan and C. Chi, *Org. Lett.*, 2012, 14, 494-497.

29. S. Chen, F. S. Raad, M. Ahmida, B. R. Kaafarani and S. H. Eichhorn, *Org. Lett.*, 2013, 15, 558-561.
30. S. More, R. Bhosale, S. Choudhary and A. Mateo-Alonso, *Org. Lett.*, 2012, 14, 4170-4173.
31. R. M. Moustafa, J. A. Degheili, D. Patra and B. R. Kaafarani, *J. Phys. Chem. A*, 2009, 113, 1235-1243.
32. B. Gao, M. Wang, Y. Cheng, L. Wang, X. Jing and F. Wang, *J. Am. Chem. Soc.*, 2008, 130, 8297-8306.
33. Y. Kou, Y.-H. Xu, Z.-Q. Guo and D.-L. Jiang, *Angew. Chem., Int. Ed.*, 2011, 50, 8753-8757, S8753/8751-S8753/8717.
34. J. Guo, Y. Xu, S. Jin, L. Chen, T. Kaji, Y. Honsho, M. A. Addicoat, J. Kim, A. Saeki, H. Ihee, S. Seki, S. Irle, M. Hiramoto, J. Gao and D. Jiang, *Nat Commun*, 2013, 4, 2736.
35. M. M. Payne, S. A. Odom, S. R. Parkin and J. E. Anthony, *Org. Lett.*, 2004, 6, 3325-3328.
36. A. Maliakal, K. Raghavachari, H. Katz, E. Chandross and T. Siegrist, *Chem. Mater.*, 2004, 16, 4980-4986.
37. M. M. Payne, S. R. Parkin and J. E. Anthony, *J. Am. Chem. Soc.*, 2005, 127, 8028-8029.
38. S.-H. Chien, M.-F. Cheng, K.-C. Lau and W.-K. Li, *J. Phys. Chem. A*, 2005, 109, 7509-7518.
39. A. Mateo-Alonso, *Chem. Soc. Rev.*, 2014, 43, 6311-6324.
40. Q. Miao, T.-Q. Nguyen, T. Someya, G. B. Blanchet and C. Nuckolls, *J. Am. Chem. Soc.*, 2003, 125, 10284-10287.
41. S.-Z. Weng, P. Shukla, M.-Y. Kuo, Y.-C. Chang, H.-S. Sheu, I. Chao and Y.-T. Tao, *ACS Appl. Mater. Interfaces*, 2009, 1, 2071-2079.
42. F. Stoeckner, R. Beckert, D. Gleich, E. Birckner, W. Guenther, H. Goerls and G. Vaughan, *Eur. J. Org. Chem.*, 2007, 1237-1243.
43. P. Totsatitpaisan, K. Tashiro and S. Chirachanchai, *J. Phys. Chem. A*, 2008, 112, 10348-10358.
44. F. S. Raad, A. a. O. El-Ballouli, R. M. Moustafa, M. H. Al-Sayah and B. R. Kaafarani, *Tetrahedron*, 2010, 66, 2944-2952.
45. G. Li, B. Zhang and Z. Wang, *Macromol. Rapid Commun.*, 2014, 35, 971-975.
46. M. Nowak, B. Kauch and P. Szperlich, *Rev. Sci. Instrum.*, 2009, 80, 046107/046101-046107/046103.
47. W. W. Wendlandt and H. G. Hecht, *Reflectance Spectroscopy (Chemical Analysis, Vol. 21)*, Inter-science, 1966.
48. S. P. Tandon and J. P. Gupta, *Phys. Status Solidi*, 1970, 38, 363-367.
49. B. C. Tlach, A. L. Tomlinson, A. G. Ryno, D. D. Knoble, D. L. Drochner, K. J. Krager and M. Jeffries-El, *J. Org. Chem.*, 2013, 78, 6570-6581.
50. S. Dalapati, S. Jin, J. Gao, Y. Xu, A. Nagai and D. Jiang, *J. Am. Chem. Soc.*, 2013, 135, 17310-17313.

*Table of Contents***Highly Porous and Photoluminescent Pyrene-Quinoxaline-Derived
Benzimidazole-Linked Polymers**

Suha Altarawneh[†], Lamia Nahar[†], Indika U. Arachchige^{*†}, Ala'a O. El-Ballouli[‡],
Kassem M. Hallal[‡], Bilal R. Kaafarani^{*‡}, Mohammad Gulam Rabbani^{†§}, Ravi K.
Arvapally[†] and Hani M. El-Kaderi^{*†}



Successful integration of pyrene-quinoxaline building units into benzimidazole-linked polymers leads to highly porous frameworks that are semiconducting and photoluminescent.

Scheme 1. Synthetic routes for **BILP-17** and **BILP-18**. (i) DMF, HCl, -30 °C, 1 hr;
(ii) DMF, 25 °C, 12 hr under N₂; (iii) DMF, 130 °C, 72 hr under O₂.

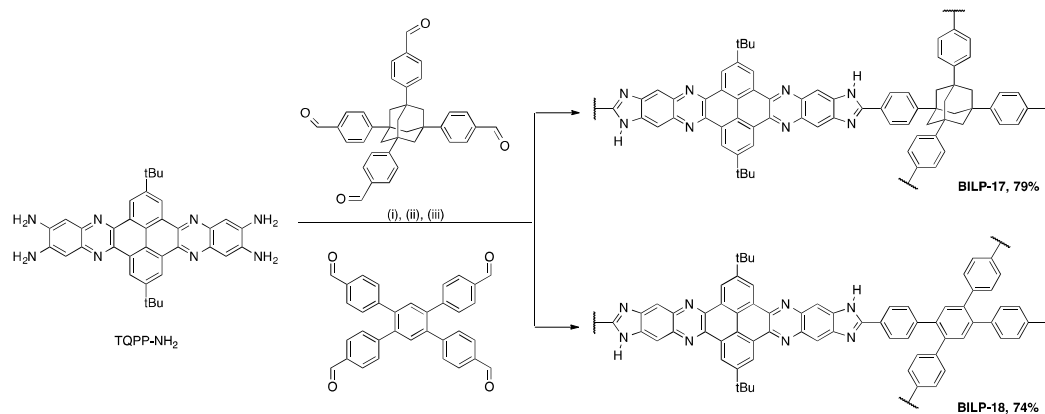


Figure 1. SEM images of **BILP-17** (A) and **BILP-18** (B); Ar isotherms (C) and pore size distributions from nonlocal density functional theory (D).

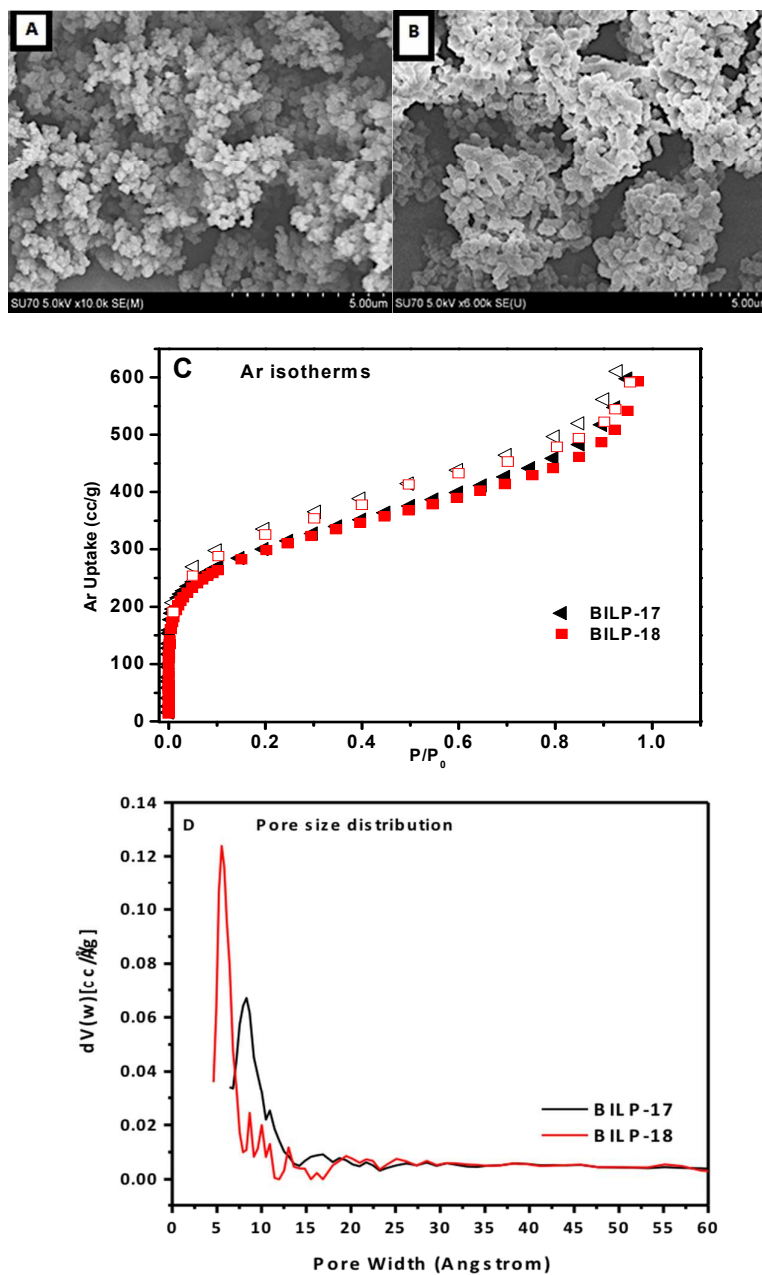


Figure 2. UV-Vis absorption (A). PLE (dotted) and PL (line) spectra of **BILP-17** (orange), **BILP-18** (red) polymers and the TQPP-NH₂ monomer unit (green) (B).

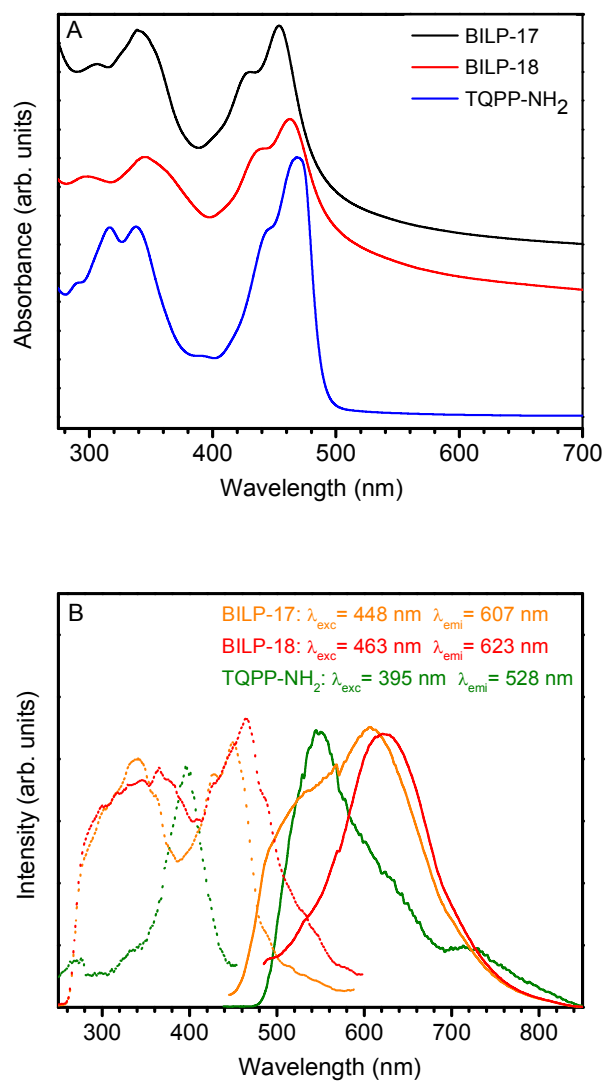


Table 1. Textural properties and bandgap values of BILPs.

Polymer	S_{ABET}^a (m² g⁻¹)	Pore Volume^b (cc g⁻¹)	Pore Size^c (Å)	Bandgap^d (eV)
BILP-17	952	0.93	8.3	2.02
BILP-18	947	0.76	5.5	2.16

^aSurface area is calculated from Ar isotherm at 87 K using the BET method, ^bPore volume is calculated from single point measurements at P/P₀ = 0.95, ^cPore size distribution is estimated from NLDFT, ^dBandgaps are calculated from solid-state diffuse reflectance spectra (converted to absorption) using Kubelka-Munk remission function.⁴⁸